Scientific Research Publishing

Materials Sciences and Applications, 2025, 16(4), 208-230
https://www.scirp.org/journal/msa
ISSN Online: 2153-1188
ISSN Print: 2153-117X

Development of Sustainable Geopolymer Binders Using Clay and Laterite from Burkina Faso with GGBFS: A Path towards Hybrid Solutions for Low-Carbon Construction

Abdoul Rachid Lankoandé[1,2], Mouhamadou Amar[2], Joelle Kleib[2], Philippe Nongwendé Ouédraogo[1,3], Lamine Zerbo[4], Mahfoud Benzerzour[2], Nor-Edine Abriak[2], Sié Kam[1*]

[1]Department of Physics, Renewable Thermal Energy Laboratory, Doctoral School of Sciences and Technologies, Joseph KI-ZERBO University, Ouagadougou, Burkina Faso
[2]Civil and Environmental Engineering Department, Civil and Geo-Environmental Engineering Laboratory, IMT Nord Europe, Lille, France
[3]Monitoring & Inspection/Structure & Environnement, Le Grand Quevilly, France
[4]Department of Chemistry, Molecular and Materials Chemistry Laboratory, Doctoral School of Sciences and Technologies, Joseph KI-ZERBO University, Ouagadougou, Burkina Faso
Email: *sie.kam@ujkz.bf

How to cite this paper: Lankoandé, A.R., Amar, M., Kleib, J., Ouédraogo, P.N., Zerbo, L., Benzerzour, M., Abriak, N.-E. and Kam, S. (2025) Development of Sustainable Geopolymer Binders Using Clay and Laterite from Burkina Faso with GGBFS: A Path Towards Hybrid Solutions for Low-Carbon Construction. *Materials Sciences and Applications*, **16**, 208-230.
https://doi.org/10.4236/msa.2025.164012

Received: March 7, 2025
Accepted: April 25, 2025
Published: April 28, 2025

Abstract

The reduction of carbon emissions from traditional cement materials, particularly Ordinary Portland Cement (OPC), remains a critical environmental challenge. This study explores the potential of locally sourced clays and laterites from Burkina Faso in the development of geopolymers as sustainable alternatives to conventional binders. The objective is to create geopolymers hardenable at room temperature using metakaolin derived from clay and laterite, while evaluating the influence of incorporating Ground Granulated Blast Furnace Slag (GGBFS) at varying levels. Different geopolymers formulations were investigated: binders based solely on clay and laterite, and two enhanced with 5% and 10% GGBFS, respectively. Microstructural analyses, including X-ray diffraction (XRD), mercury intrusion porosimetry, and Fourier transform infrared spectroscopy (IRFT), were conducted to assess the stability and performance of the formulations. The results reveal the formation of amorphous mineral phases, as well as a significant improvement in mechanical strength reaching 300% and 160% respectively for clay and laterite-based formulations, following the incorporation of 10% GGBFS, compared to formulations without GGBFS. In addition, a reduction in porosity of the order of 28% for clay formulations and 45% for hybrid clay/laterite formulations was observed with

the addition of 10% GGBFS compared to formulations without this addition. Geopolymers based on Burkina Faso's clay and laterite, with or without GGBFS, demonstrate strong potential as low-carbon alternatives to OPC.

Keywords

Clay, Laterite, Ground Granulated Blast Furnace Slag (GGBFS), Geopolymer Paste, Low-Carbon Binders

1. Introduction

The construction industry is a major contributor to global pollution, particularly through CO_2 emissions. Concrete, largely dependent on Ordinary Portland Cement (OPC), is at the heart of this issue [1]. OPC production not only releases vast amounts of greenhouse gases but also consumes millions of tons of natural resources annually, driving deforestation, ecosystem degradation, and industrial waste accumulation [2]. Addressing these challenges is crucial to shaping the future of sustainable construction [3].

Geopolymers have emerged as a viable, eco-friendly substitute for OPC [4]-[6]. Unlike OPC, geopolymers rely on industrial by-products such as Ground Granulated Blast Furnace Slag (GGBFS) and fly ash, significantly reducing waste and resource extraction [7]-[9]. Their polymeric structure, formed through the alkaline activation of aluminosilicate minerals, imparts superior mechanical properties, durability, and resistance to harsh environments all while minimizing their carbon footprint [10] [11]. A variety of raw materials, including kaolin clay and laterite, have been explored for geopolymer synthesis due to their abundance and aluminosilicate content [12]-[14]. Studies reveal that thermally activated clays, particularly metakaolin, enhance the reactivity and performance of geopolymers [15] [16]. Similarly, calcined laterite, rich in iron oxides and alumina, has demonstrated promising mechanical properties, making it suitable for low-cost, sustainable construction, especially in regions with limited access to traditional building materials [17] [18]. Burkina Faso, endowed with abundant clay and laterite deposits, offers a unique opportunity to develop geopolymers tailored to local conditions. Traditionally used in construction [19], these materials can be transformed into high-performance binders. Metakaolin derived from clay provides a rich source of aluminosilicates, while laterite enhances mechanical strength due to its high iron oxide and alumina content [20] [21]. Incorporating GGBFS further strengthens these binders and enhances their chemical stability, providing a practical and sustainable alternative to Portland cement [22] [23].

This study investigates the formulation and characterization of geopolymer binders using clay, laterite, and blast furnace slag. It explores the effects of partially substituting clay with laterite on the physico-chemical and mechanical properties of geopolymers, with the aim of developing high-performance, eco-friendly binders at moderate temperatures. By leveraging local materials and industrial waste,

this research addresses the dual challenge of reducing construction's carbon footprint and managing resources responsibly. The results could pave the way for a new generation of sustainable building materials, aligning performance with environmental stewardship. This work highlights the potential of geopolymers to transform the construction sector in Burkina Faso and beyond, promoting environmentally friendly infrastructure development.

2. Materials and Methods

2.1. Raw Materials

The materials used in this study included crushed Ground Granulated Blast Furnace Slag (GGBFS), calcined clay (MKC: Calcined Clay Material), calcined laterite (MKL: Calcined Lateritic Material) and an Alkaline silicate (ALK) brand Geosil. Alkaline silicate, manufactured by Woellner, is a potassium-based geopolymer reagent, essential for alkaline activation. The GGBFS, a by-product of steel operations, were supplied by the Ecocem plant in Dunkerque, France, in a process of recovering industrial waste. The clay and laterite used to produce MKC and MKL were extracted respectively from the Burkinabe careers of Sitiéna (10˚36'15"N, 4˚48'18"W) and Dayoubsi (12˚14'35"N, 1˚37'09"W), areas where these materials are abundant and traditionally used for local construction. These local resources were chosen for their relevance in the context of sustainable construction in West Africa, helping to reduce the carbon footprint associated with the import of materials. The clay and laterite materials were thermally activated at 650˚C for 2 hours and 30 minutes in a Nabertherm LH 30/14 furnace, following a preliminary grinding using a **Retsch SR 300 impact crusher** to enhance their reactivity. This grinding process resulted in a maximum particle size of **250 µm,** thereby ensuring their suitability for the geopolymerization process (Figure 1).

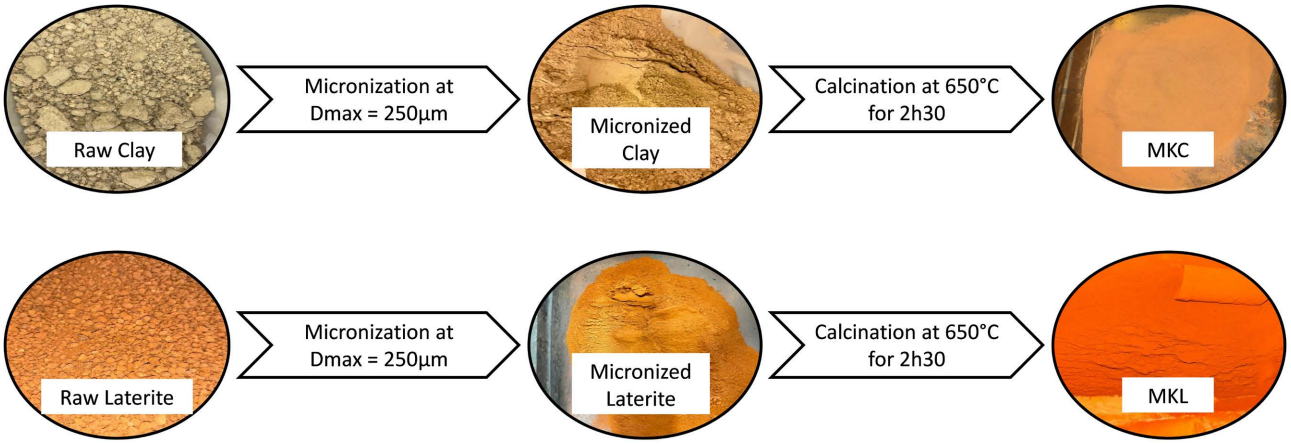

Figure 1. Diagram illustrating the sequential stages involved in the preparation of clays and laterites for their subsequent utilization.

The formulations developed in this study are divided into three groups, differentiated by the composition of the geopolymer binders. The first group of formulations is based on clay (MKC), with the addition of different percentages of

GGBFS (0%, 5% and 10%), corresponding respectively to the references MKC0, MKC5 and MKC10. For example, in MKC0, the number "0" indicates that no GGBFS have been added. The second group concerns laterite-based formulations (MKL), following the same percentages of GGBFS and designated by MKL0, MKL5 and MKL10. The latter group combines the two sources of aluminosilicates, clay (MKC) and laterite (MKL), with the same adjustments in GGBFS. The associated references are MKLC0, MKLC5 and MKLC10. For example, MKLC5 contains 47.5% MKL, 47.5% MKC, and 5% GGBFS. In total, nine distinct formulations were developed, with a constant alkaline/binder ratio (ALK/B) of 0.5 and a water/binder ratio (W/B) of 0.06. These formulations are summarized in Table 1.

Table 1. Mixing proportions for geopolymer pastes.

	ALK/B	MKC (%)	MKL (%)	GGBFS (%)	W/B
MKC0	0.5	100	00	00	0.06
MKC5	0.5	95	00	05	0.06
MKC10	0.5	90	00	10	0.06
MKL0	0.5	100	00	00	0.06
MKL5	0.5	95	00	05	0.06
MKL10	0.5	90	00	10	0.06
MKLC0	0.5	50	50	00	0.06
MKLC5	0.5	47.5	47.5	05	0.06
MKL10	0.5	45	45	10	0.06

2.2. Experimental Methods

The pastes were prepared by mixing the aforementioned materials in different proportions, following a specific mixing protocol that corresponds to the promising results obtained in previous studies by Alloul *et al.* [24] [25]. This protocol included a meticulous procedure designed to achieve optimal mixing. The paste preparation process was rigorously structured as follows: first, the materials were accurately weighed, followed by the start-up of the mixer. Next, the less reactive aluminosilicates (MK) were added progressively to ensure uniform distribution, with a mixing time of 5 minutes for formulations incorporating both clay MK (MKC) and laterite (MKL). The liquid solution was then poured slowly for 5 minutes. Finally, the most reactive binder, GGBFS, was incorporated and mixed for 3 minutes to initiate the critical geopolymerization processes. The paste mixture was then poured into molds and placed on a vibrating table to ensure compaction and eliminate air bubbles. Sealing the molds for the first 24 hours is crucial to initiating the curing process, allowing the pastes to mature and gain strength at room temperature. These steps, carried out systematically, are intended to ensure a careful preparation of the paste, taking into account key factors such as mixing time, compaction and hardening. These elements are essential for the proper eval-

uation of the properties and performance of geopolymer materials.

The prepared paste was subjected to a full series of tests to evaluate their intrinsic properties. The compressive strength tests were carried out on 35 × 40 mm cylindrical test pieces, using an INSTRON 5500 R universal test machine, which complies with the NF EN 196-1 standard [25]. These tests were carried out at a loading speed of 0.5 mm/min, according to the specifications of the standard to ensure reproducible results.

The analysis technics included several physical and chemical methods to characterize the materials. The density of the materials was measured using a Micromeritics AccuPyc 1330 device, using the gas displacement method (He) at a pressure of 1 bar and a temperature of 25˚C. The BET area was determined from the nitrogen adsorption/desorption analysis, performed with a Micromeritics 3 Flex analyzer, using a pressure range of 0.05 to 0.1 p/p° to obtain accurate measurements. The porosity accessible to mercury was measured with the AutoPore V-905 device, applying a pressure ranging from 0.003 to 205 MPa, thus allowing a detailed analysis of the distribution of pore sizes.

Differential thermal analysis (DTA) and thermogravimetric analysis (TGA) were carried out using a NETZSCH STA 449 F3 Jupiter instrument coupled to the QMS 403 Aëolos Quadro mass spectrometer. The protocol included heating at 2˚C /min from 40˚C to 105˚C, followed by ramping at 3˚C/min from 105˚C to 1000˚C, providing in-depth analysis of thermal reactions and mass losses.

X-ray diffraction (XRD) was carried out using a Bruker D2 diffractometer equipped with a Cu Kα tube, with a resolution of 0.02˚ and a range of diffraction angles (2θ) ranging from 5˚ to 80˚, to determine the crystalline structure of the materials. X-ray fluorescence (FX) was carried out with a Bruker S2 RANGER device, using an X-ray beam with an energy of 50 kV and an intensity of 30 mA, allowing the qualitative and quantitative analysis of the elements present. Finally, Fourier transform infrared spectroscopy (IRFT) was performed with a Thermo Scientific Nicolet iS20, with 32 scans and a resolution of 4 cm^{-1}, to study the molecular vibrations of the functional groups present.

The reactivity of the materials and the heat release were evaluated by calorimetry with isothermal heat flux at 20˚C, using a custom calorimeter equipped with flow meters for rapid balancing of the samples (in 5 minutes). This measurement made it possible to track heat variations during the early stages of geopolymerization, which is crucial for understanding reaction kinetics.

These analytical techniques, with their detailed application conditions, have collectively made it possible to better understand geopolymerization reactions, hydration products and interfacial bonding in paste structures.

3. Results and Discussion

3.1. Raw Materials Characterization

Physical characterization of the materials used revealed a minimum density of 2.71 g/cm^3 for GGBFS, and BET area of 36.74 m^2/g for MKL. **Table 2** shows the

FX analysis of the materials, indicating the mass percentages of SiO_2 and Al_2O_3: 68.62% for MKC, 50.25% for MKL, and 44.71% for GGBFS.

Table 2. Physical and chemical composition of the materials used.

Chemical composition (%)	GGBFS	MKC	MKL
SiO_2	31.87	50.64	29.77
Al_2O_3	12.84	17.98	20.48
Fe_2O_3	0.43	13.47	46.64
CaO	39.73	3.07	0.20
MgO	10.00	4.00	-
K_2O	-	-	0.50
Na_2O	-	5.30	-
Physical characteristics			
Density (g/cm^3)	2.71	2.84	3.12
Specific BET area (m^2/g)	33.01	16.62	36.74

The X-ray diffraction analysis (**Figure 2**) made it possible to identify the mineral phases present in the raw materials and after calcination. The raw lateritic material is mainly composed of kaolinite, nacrite, goethite, hematite and quartz, which is typical of laterites rich in iron and alumina. After calcination, MKL (calcined laterite) mainly has hematite, nacrite and quartz. The persistence of hematite indicates the thermal stability of iron oxides, according to Cornell & Schwertmann studies reported by Bowles [26] on iron oxides.

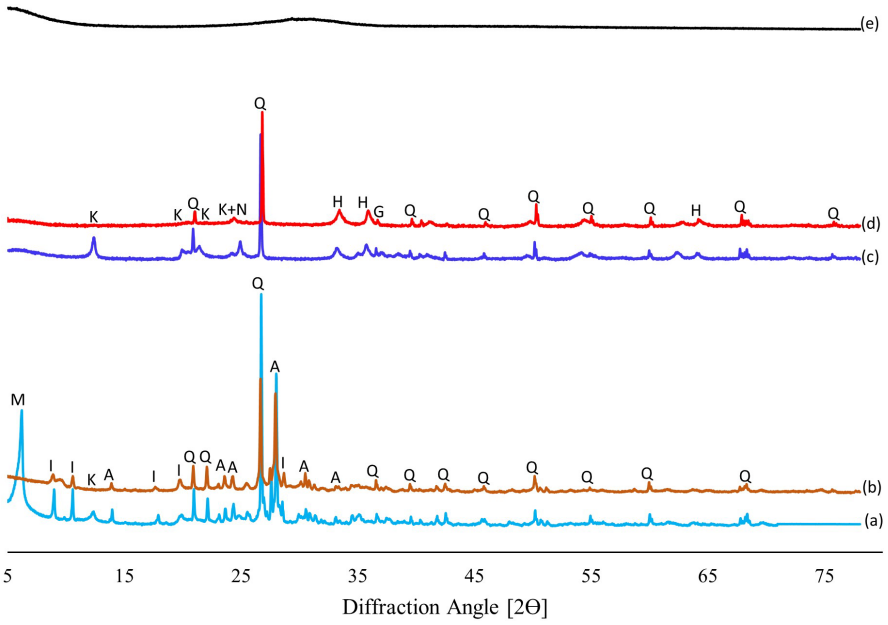

Figure 2. XRD spectra of raw clay (a), MKC (b), raw laterite (c), MKL (d) and GGBFS (e): M = Montmorillonite; I = Illite; K = Kaolinite; A = Albite; N = Nacrite; Q = Quartz; G = Goethite and H = Hematite.

Similarly, the raw clay material consists of kaolinite, albite, illite, montmorillonite and quartz. Calcination eliminates the hydroxylated phases (kaolinite and montmorillonite), leaving a material mainly composed of albite, illite and quartz. The disappearance of the hydroxylated phases is due to thermal dehydroxylation, a phenomenon consistent with the work of Soré *et al.* [20] on the transformation of clay minerals.

As for the GGBFS, it is distinguished by an amorphous structure characterized by a halo between 25˚ and 35˚ 2θ. This amorphous structure is characteristic of blast furnace lats, as described by Alloul *et al.* [24] in their work geopolymer materials.

The infrared spectra (**Figure 3**) corroborates the observations of the XRD analysis, providing additional information on the mineralogical composition of the materials. The characteristic bands of the mineral phases, such as the Al-OH bond of clays (between 3600 and 3700 cm^{-1} for kaolinite, illite and montmorillonite), are observed, which is consistent with the studies of Dah-Traoré *et al.* [27] on the IR spectra of clay minerals. The band around 913 cm^{-1} is typical of the Al-O bonds of kaolinite, as shown by the work of Sanou *et al.* [28] and Ramadji *et al.* [29]. The 797 - 778 cm^{-1} double band confirms the presence of quartz while the 762 cm^{-1} band is associated with albite, which is consistent with McKeown [30] spectral data on the IR spectrums of albits.

The transformation of kaolinite into metakaolinite is evidenced in the infrared spectra of MKC and MKL. This transition is confirmed by the disappearance of the characteristic bands of kaolinite in the range of 3620 – 3700 cm^{-1}, as well as by the absence of the typical doublet of kaolinite at 913 cm^{-1}, which is consistent with the observations of Soré *et al.* [20] and Seynou *et al.* [31] on the dehydroxylation of kaolinite.

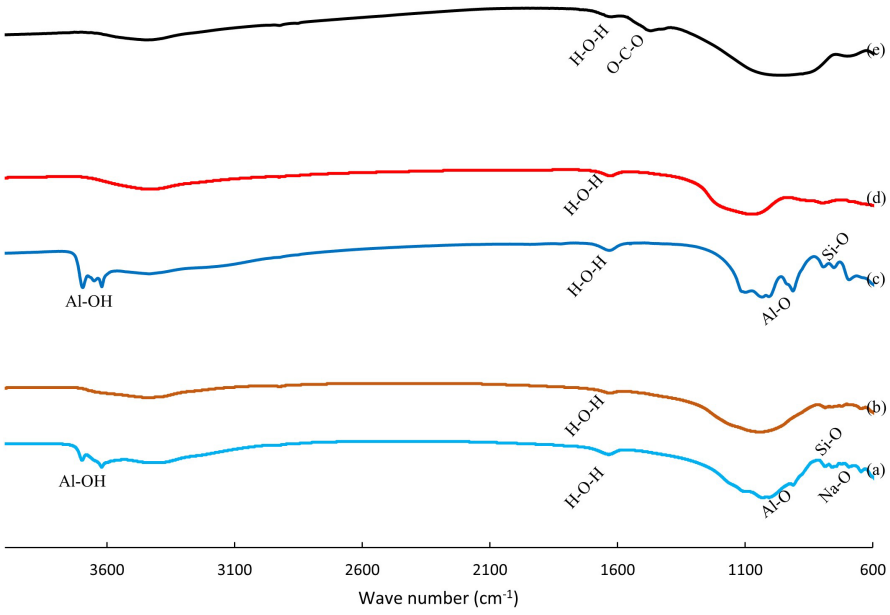

Figure 3. IRFT spectra of raw clay (a), MKC (b), raw laterite (c), MKL (d) and GGBFS (e).

The band at 1632 cm^{-1} results from the H-O-H flexion vibrations of the absorbed water molecules, a phenomenon studied by Elimbi *et al.* [32] and Tchakoute *et al.* [33] on the IR spectra of metakaolins. Finally, a carbonate signature at 1480 cm^{-1} is observed for the GGBFS, which is expected given the presence of carbonates in the blast furnace milkman, as discussed by Finnocchiaro *et al.* [34].

The thermal analysis (**Figure 4**) was carried out to identify the specific transformations of the raw materials, focusing on their relevance for geopolymerization. Our results reveal for raw clay a double endothermic peak between 140˚C and 310˚C, a peak corresponding to the dehydroxylation of montmorillonite. This double peak, compared to Emmerich's [35] studies that deal with dehydroxylation, suggests a possible complex structure of montmorillonite in our clay.

This double peak is followed by a major peak between 380˚C and 700˚C, attributable to kaolinite. The position and intensity of this peak are consistent with studies by Elimbi *et al.* [32] and Castelein *et al.* [36] who studied the dehydroxylation of kaolinite in similar materials. For raw laterite, a minor peak between 240˚C

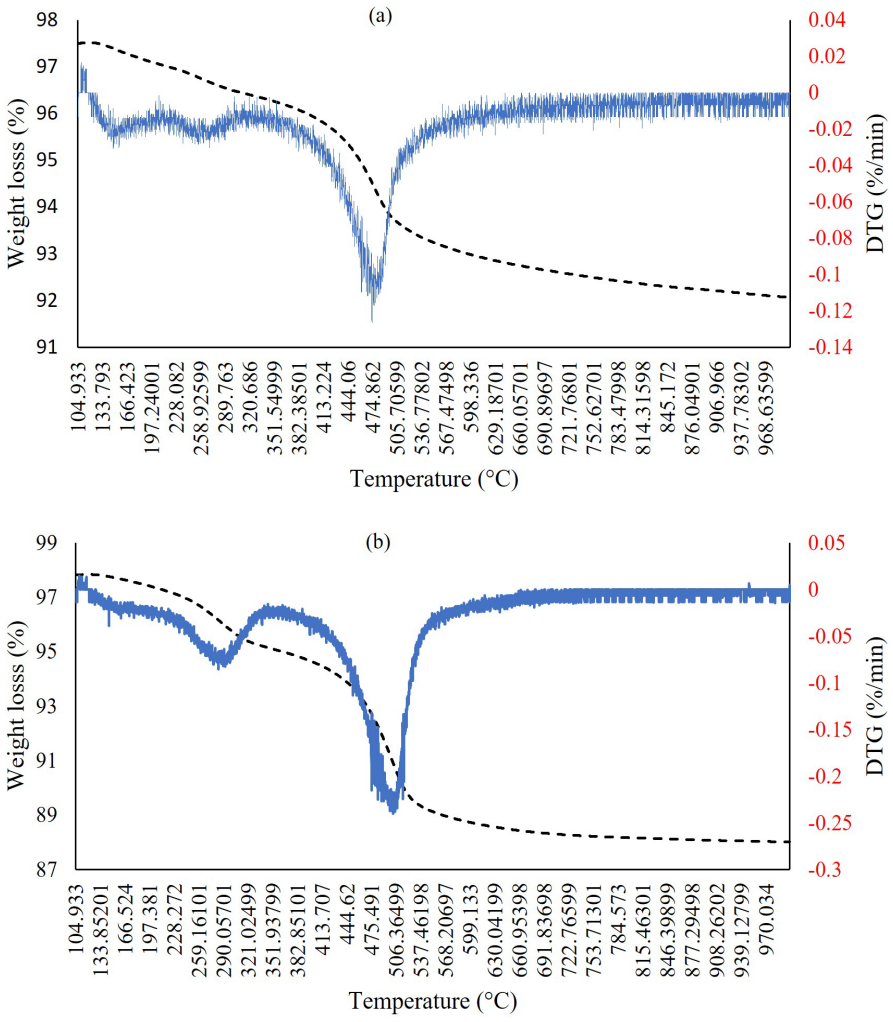

Figure 4. TGA/DTA analysis of raw clay (a) and raw laterite (b).

and 325˚C indicates the transformation of goethite into hematite, a transformation often observed in iron-rich laterites, as discussed by Wolska and Schewertmann [37]. This minor peak, compared to these studies that deal with the dehydration of goethite, suggests a possible low proportion of goethite in our laterite. This minor peak is followed by a major peak between 380˚C and 700˚C, reflecting the dehydroxylation of the kaolinitic phases. The similarity of this peak with that observed for raw clay indicates a significant presence of kaolinite in laterite.

These results highlight the potential of MKC and MKL materials as sources of aluminosilicates, essential for geopolymerization, a process discussed by Davidovits [38] in his fundamental work. The presence of ferric oxides, especially in MKL, could also help improve the mechanical properties of formulated geopolymers. However, a more in-depth analysis of the kinetics of these transformations, using techniques such as differential scanning calorimetry (DSC) at variable heating speeds, could provide additional information on the reactivity of raw materials.

3.2. Mass Loss after Curing

The mass losses of the different formulations were evaluated in this study. **Figure 5** illustrates these mass losses as a function of the partial substitution of metakaolin (MK) by granulated blast furnace milk (GGBFS). A decrease in mass losses was observed with the increase in the substitution rate, which can be attributed to two main antagonistic phenomena.

The first phenomenon is the modification of the granular skeleton of solid particles (MKC, MKL and GGBFS). GGBFS leads to the formation of a denser and less porous structure during its polymerization. A mass substitution of the MK by the GGBFS leads to an increase in the number of particles in the same volume. This leads to a less porous granular mixture, capable of absorbing a smaller amount of water during the preparation of the paste [38]. This reduction in initial porosity can limit the amount of water available for subsequent evaporation, thus contributing to the reduction of mass losses.

The second phenomenon concerns the decrease in the level of ferric oxide in the geopolymeric matrix with the addition of GGBFS (0.43% iron oxide in GGBFS compared to 13.47% for MKC and 46.64% for MKL). Sore *et al.* [20] and Ishikawa *et al.* [39] have shown that increased iron oxide content improves shrinkage resistance, thus limiting weight loss. Although the variation in iron oxide content is relatively small in this study, it could nevertheless explain some of the differences observed in mass losses. For example, the MKL0 sample, which contains 46.64% iron oxide, lost only 1.5% of its mass, while the MKLC0 sample, with only 30.05% iron oxide, lost 1.7%. This observation suggests that the iron oxide content, although modest, plays a role in the dimensional stability of geopolymers.

The formulations composed only of MKC and GGBFS have the maximum mass loss, followed by those containing MKLC and GGBFS. The substitution of 10% MK by GGBFS results in a minimum mass loss, regardless of the type of geopoly-

mer. This trend indicates that the addition of GGBFS leads to a more stable microstructure and less prone to water loss.

Weight loss can mainly be explained by the evaporation of the water contained in the alkaline solution, initially absorbed by the raw materials [20]. This significant evaporation could lead to shrinkage and cracking of the samples, thus affecting their structural integrity. The reduction of mass losses with the addition of GGBFS therefore suggests better water retention and a more shrinkage-resistant microstructure.

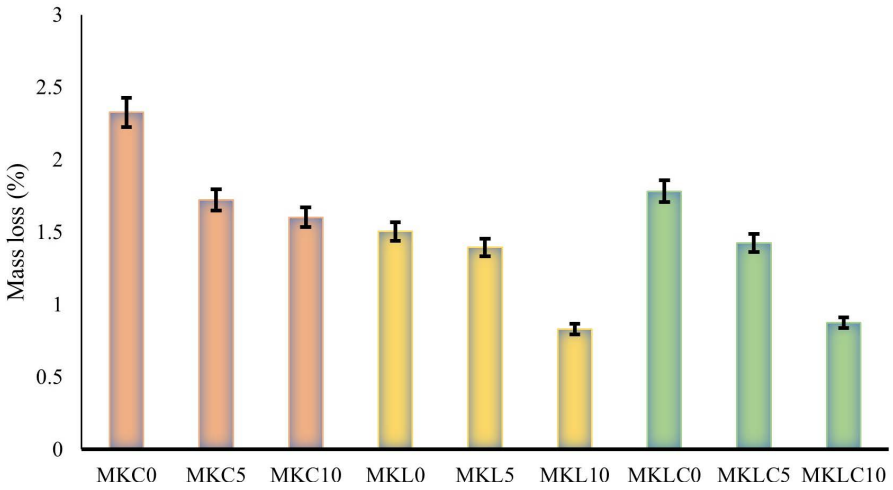

Figure 5. Mass loss % for geopolymer binders after 7-day curing time.

3.3. Compressive Strength Test

Figure 6 illustrates the variation in the compressive strength of geopolymers according to their different compositions. A significant increase in compressive strength is observed when 10% of MKC or MKL is replaced by GGBFS. This trend is verified for the three types of formulations tested: clay-based formulations, laterite-based formulations and mixed formulations. The GGBFS acts as an accelerator of the geopolymerization reaction, strongly influencing the mechanical properties [40].

The improvement in compressive strength with the increase in GGBFS can be attributed to the rapid uptake and hardening of reactive aluminosilicate species and their polycondensation, which strengthens the geopolymeric gel matrix. This densification of the microstructure, induced by the GGBFS, reduces porosity and increases cohesion, which results in increased resistance, a phenomenon also observed by Bernal *et al.* [41] in their studies on dairy-based geopolymers.

MK geopolymers have seen their mechanical strength triple with the incorporation of GGBFS (from 3.08 MPa to 9.62 MPa), although this resistance remains low compared to that of MKL and MKLC geopolymers, whose compressive strengths have increased with the GGBFS content. These results corroborate the studies of Kaze *et al.* [42], who studied the performance of iron-rich calcined laterite for the formulation of geopolymers, obtaining a good compressive strength

for samples dried at 20˚C.

In addition, Steveson *et al.* [43] showed that the ideal molar ratio of SiO_2/Al_2O_3 to optimize compressive strength is between 3.5 and 3.8. However, our results, as highlighted in **Figure 6** and **Table 3**, show a slight deviation from those of this study. The MKC and GGBFS geopolymers, characterized by a molar ratio of SiO_2/Al_2O_3 ranging from 2.78 to 2.82, have lower compressive strengths compared to the MKL and GGBFS geopolymers as well as the MKLC and GGBFS geopolymers. Indeed, these latter geopolymers have SiO_2/Al_2O_3 molar ratios ranging from 1.45 to 1.55 for MKL and GGBFS, and from 2.13 to 2.17 for MKLC and GGBFS.

This deviation could be attributed to the highly crystalline nature of MKC- and GGBFS-based geopolymers, which contain a significant proportion of unreacted albite ($NaAlSi_3O_8$) despite heat treatment. This residual crystallinity limits the formation of amorphous geopolymeric gel, which is responsible for mechanical resistance. On the other hand, the MKL and GGBFS geopolymers and MKLC and GGBFS demonstrate improved reactivity and structural development [44].

The best molar ratio for improved compressive strength in our case is 2.17, corresponding to the MKLC10 formulation (addition of 10% GGBFS). Previous research has shown that an increase in SiO_2 content can significantly reduce the long-range structural order, promoting the formation of disordered geopolymeric structures and improving compressive strength [44]. This is consistent with the more amorphous nature of the MKLC samples observed in their XRD diagrams (presence of halo peaks) and the fact that these samples have the best compressive strengths. This correlation between amorphization and mechanical resistance has been widely documented in the literature, in particular by Palomo *et al.* [45].

Table 3. Molar ratio SiO_2/Al_2O_3 of different formulations.

Formulations	MKC0	MKC5	MKC10	MKL0	MKL5	MKL10	MKLC0	MKLC5	MKLC10
Molar ratio SiO_2/Al_2O_3	2.82	2.80	2.78	1.45	1.50	1.55	2.13	2.15	2.17

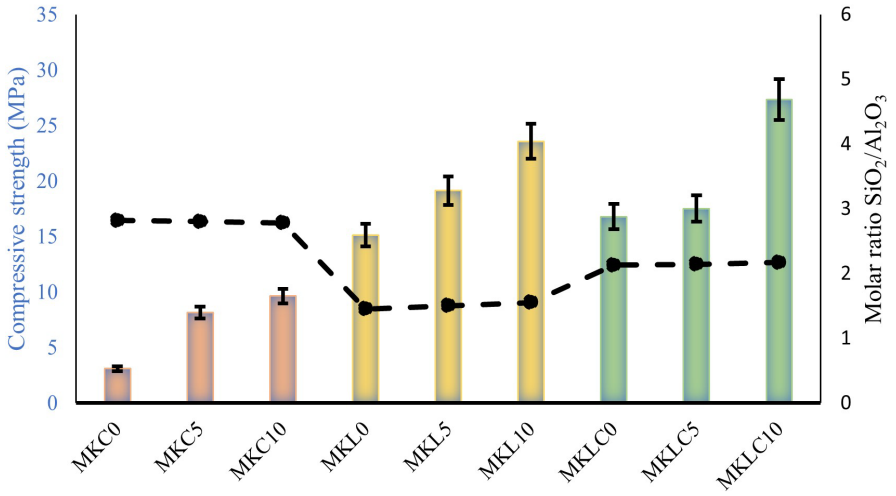

Figure 6. Compressive strength (MPa) on day 7 according molar ratio SiO_2/Al_2O_3.

We can deduce that the addition of a small proportion of GGBFS (about 5 to 10%) to the MK provides an additional amount of amorphous silica, promoting the production of a significant amount of geopolymeric gel. This addition improves the mechanical properties of geopolymeric binders [24]. This increase in amorphous silica, in addition to the densification due to C-A-S-H, contributes to the compact and resistant microstructure.

3.4. Mercury Porosity

The mercury porosity analysis was carried out using our different formulations to characterize their porous structure. Only geopolymers with the best properties (compressive strength and mass loss) were selected for these tests. The results reveal significant differences in the distribution of porosities, making it possible to evaluate the impact of the addition of granulated blast furnace milk (GGBFS) on the properties of geopolymer binders.

Measurements indicate high porosity levels, ranging from 15.43% for MKLC10 to 23.69% for MKL0. These variations in porosity directly reflect the modification of the microstructure of the geopolymer as a function of the addition of GGBFS. Higher porosity, as observed for MKL0, suggests a less dense and potentially more permeable structure, which can negatively affect the durability of the material by facilitating the penetration of aggressive agents, a phenomenon also observed by Collins and Sanjayan [46] in their studies on geopolymer durability.

The total pore surfaces of the different geopolymers reveal that MKL0, MKL5, MKL10, MKLC0, MKLC5 and MKLC10 have respectively total pore surfaces of 38.45 m^2/g, 32.18 m^2/g, 27.40 m^2/g, 43.39 m^2/g, 31.49 m^2/g and 23.90 m^2/g. The decrease in the total area of the pores with the increase in the percentage of GGBFS indicates a densification of the microstructure, potentially due to the formation of additional phases or the filling of existing voids.

These results, in conjunction with those of mechanical characterization, reveal a significant correlation between the volume of pores accessible to mercury and the compressive strength. A notable observation has been made: as the percentage of GGBFS increases from 0% to 5%, then to 10% in the formulations studied (MKL0, MKL5, MKL10, MKC0, MKC5, MKC10, MKLC0, MKLC5 and MKLC10), the compressive strength increases while the porosity is accessible to mercury decreases. For example, MKLC10 had a significantly higher compressive strength and a significantly lower mercury-accessible porosity compared to MKLC0 and MKLC5, with increases of 63% and 4% in compressive strength, respectively, and decreases of 8% and 4% in mercury-accessible porosity.

Thus, it is clearly established that the increase in the percentage of GGBFS in the geopolymer formulations leads to a reduction in porosity and a concomitant improvement in compressive strength. This inverse relationship between porosity and mechanical strength suggests that GGBFS contributes to the formation of a more compact and homogeneous microstructure, a phenomenon widely documented in the literature on geopolymers [47].

Previous studies have also indicated that the addition of GGBFS can reduce porosity and improve the microstructure of geopolymers by forming a C-A-S-H gel that fills voids and improves the compressive strength of mortars [24] [48]. This C-A-S-H gel, in addition to the aluminosilicate gels formed during geopolymerization, contributes to the densification of the matrix and the reduction of porosity. Figure 7 illustrates the impact of the incorporation of GGBFS on the porosity of different geopolymers.

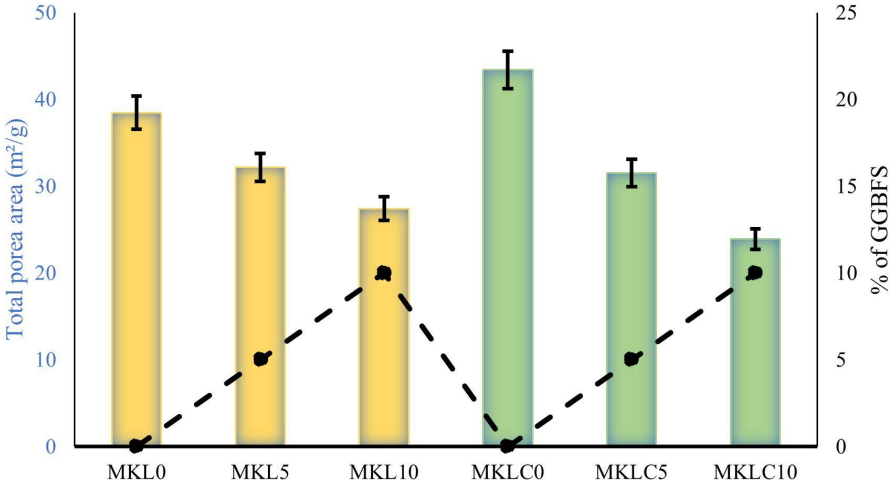

Figure 7. Impact of the addition of GGBFS on porosity.

3.5. IRFT

Fourier transform infrared spectroscopy (IRTF) of geopolymers generates spectral bands resulting from the interaction between the material and infrared radiation [49]. These bands correspond to specific bonds and atomic groups present in the material, thus making it possible to decipher its molecular composition. This technique provides an overview of the three-dimensional structural network of the material, highlighting the strong atomic bonds involving mainly aluminum (Al), silicon (Si) and oxygen (O).

The results are presented in Figure 8, illustrating the spectral bands identified during these tests. The IRTF analysis of our different geopolymer formulations (MKC, MKL and MKLC) reveals similar peaks in all families, which is consistent with the observations of Kaze *et al.* [42] on similar geopolymers. However, slight variations in intensity and width are observed, some peaks being more pronounced than others, suggesting differences in the microstructure and composition of the formulations. The vibrations of the bound water molecules were recorded at 1632 cm^{-1} and between 3100 - 3690 cm^{-1}, attributed respectively to deformation (H-O-H) and elongation (-OH) [33] [50] [51]. These peaks indicate the presence of residual water in the structure, which can influence the porosity and therefore the mechanical resistance of the geopolymer. The silicate structure is characterized by the main peak located at 1000 cm^{-1}, linked to the vibration of the Si-O/Al-O bond of the aluminosilicate structure, reflecting the formation of the

amorphous aluminosilicate gel [52] [53]. The intensity and width of this peak can be correlated with the degree of polymerization and the formation of the geopolymeric phase, directly impacting the compactness and durability of the material.

It is interesting to note the presence of intensity due to the influence of carbonates, located at 1380 cm^{-1}, in particular for the formulations incorporating granulated blast furnace milk (GGBFS) (MKL5, MKL10, MKC5, MKC10, MKLC5 and MKLC10), corresponding to the elongation vibrations of the O-C-O bonds in the carbonate group due to the carbonation reaction [24] [33] [54]. The presence of carbonates can modify the microstructure, potentially by increasing the density and reducing the porosity, which can positively influence the compressive strength. However, excessive carbonation can also lead to long-term embrittlement of the material.

These distinct characteristics collectively demonstrate the precise formation of a geopolymer structure, reaffirming the integrity and complexity of the material's atomic bonds. By correlating variations in peak intensity and width with macroscopic properties, such as compressive strength and porosity, we can better understand how the microstructure affects the performance of the geopolymer.

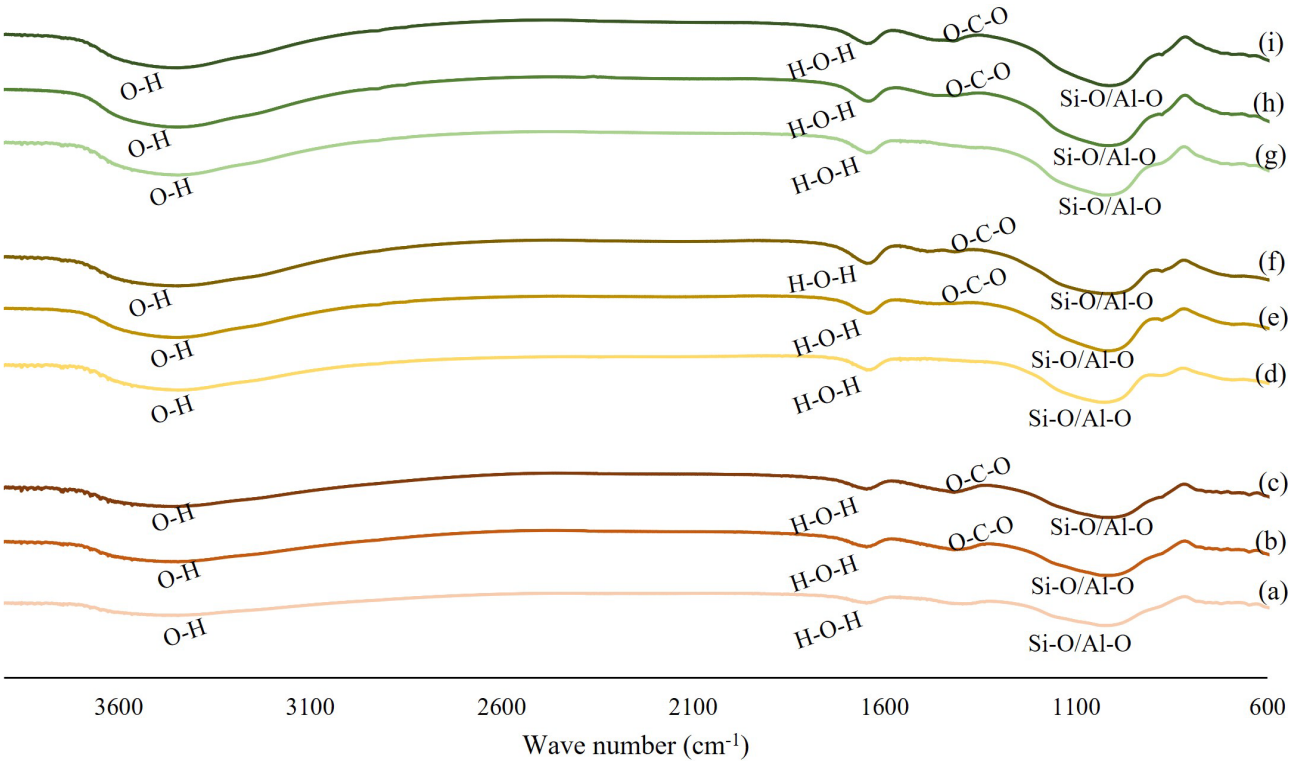

Figure 8. IRFT spectra of MKC0 (a), MKC5 (b), MKC10 (c), MKL0 (d), MKL5 (e), MKL10 (f), MKLC0 (g), MKLC5 (h) and MKLC10 (i) after 7 days curing.

3.6. XRD

Figure 9 shows the X-ray diffraction (XRD) analysis of the different formulations of geopolymer linders after 7 days of cure. The results reveal that the samples of

each family (MKC, MKL and MKLC) have similar mineralogical compositions, mainly identifying phases of quartz, albite, illite, nacrite and hematite. The presence of these residual crystalline phases indicates that the geopolymerization reaction has not completely dissolved the original minerals, which is common in metakaolin-based geopolymers.

It is particularly interesting to note that some formulations, in particular MKLC5 and MKLC10, display lower intensities for albite and hematite peaks. This decrease in intensities can be interpreted as a sign of significant rearrangements of the mineral structures of the constituent materials (MKC, MKL and GGBFS) during the geopolymerization reaction. The formation of new less orderly networks, typical of amorphous geopolymeric gels, would explain the reduction in the intensity of these crystalline peaks.

This microstructural transformation could potentially influence the mechanical properties and durability of the geopolymer, since a decrease in crystallinity can often be associated with an increase in porosity and a change in compressive strength, as shown by studies by Duxson *et al.* [47] on structure-property relationships in geopolymers.

In addition, the continuous presence of quartz, although less reactive, can act as a reinforcement phase in the geopolymeric matrix. The distribution and shape of quartz crystallites could thus affect the abrasion resistance and hardness of the material. Illite and nacrite, as clay minerals, contribute to the cohesion and plasticity of the initial mixture, but their transformation into amorphous geopolymeric phases is crucial for the development of binding properties.

The results of this study are consistent with the conclusions of previous studies on the complete non-alteration of the crystalline phases present in raw materials during the development of metakaolin-based geopolymers (MK) [6] [24] [55].

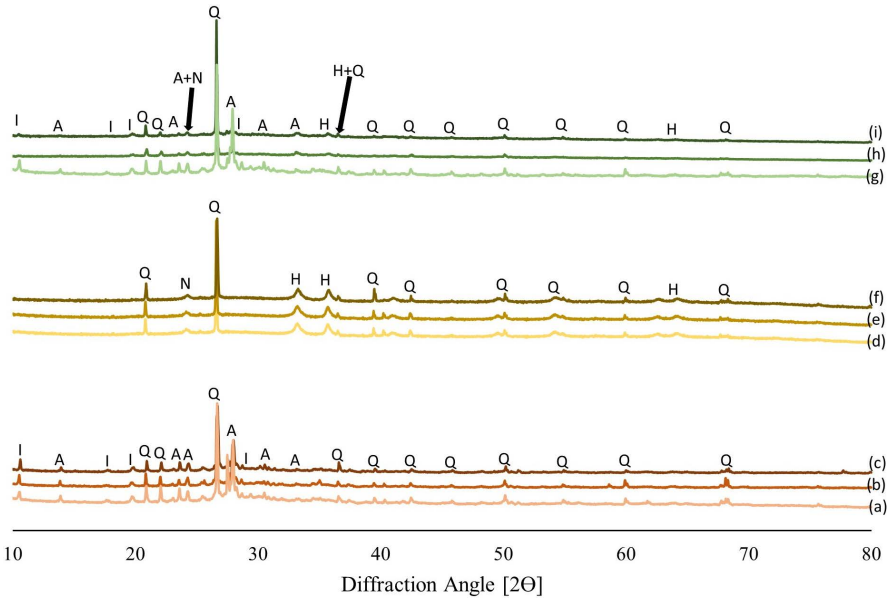

Figure 9. XRD of MKC0 (a), MKC5 (b), MKC10 (c), MKL0 (d), MKL5 (e), MKL10 (f), MKLC0 (g), MKLC5 (h) and MKLC10 (i) after 7 days curing.

However, the analysis of peak intensity variations, as observed for MKLC5 and MKLC10, makes it possible to qualify this statement and highlight significant microstructural rearrangements. A more in-depth analysis of peak widths, and the study of changes in the shape of peaks, could make it possible to better quantify phase changes and correlate these changes with the macroscopic performance of geopolymers, as suggested by the work of Provis and van Deventer [56] on the quantitative analysis of phases in geopolymers.

3.7. Calorimetry

The geopolymer groups with the best compressive strength and minimum mass loss were selected for the heat flow tests. **Figure 10** illustrates the evolution of this flow in metakaolin-based geopolymer pastes (MK) with variable percentages of incorporation of granulated blast furnace milk (GGBFS).

A significant exothermic peak is observed immediately after the material is mixed with the activator. This heat release is associated with the wetting and dissolution of the aluminosilicate precursor [57]. This initial step is crucial for the release of the reactive species that will form the geopolymeric gel. At this point, the MKLC10 and MKL10 samples have a higher heat rate among all pastes, which suggests that a high rate of MK substitution by GGBFS accelerates the dissolution behavior of metakaolin [58] [59]. This rapid dissolution indicates greater availability of reactive species, which can potentially lead to faster and denser frost formation.

The appearance of a second weak exothermic peak in MKLC5, MKL5, MKLC10 and MKL10 pastes, as indicated, highlights the formation and polymerization of gels [60] [61]. This second peak represents the geopolymerization reaction itself, where the dissolved species condense to form the three-dimensional gel network, a mechanism detailed by Davidovits [62] in his fundamental work on geopolymers. This two-step heat-release behavior was also observed in sodium silicate-activated metakaolin geopolymer pastes, as reported by other studies [63]-[65]. The presence of this second peak confirms the formation of the geopolymeric phase and can be correlated with the final mechanical strength of the material, as demonstrated by the studies of Palomo *et al.* [45] on the kinetic-property relationships in geopolymers.

Unlike MKLC5, MKL5, MKLC10 and MKL10 pastes, MKLC0 and MKL0 samples have a lower heat content and no noticeable thermal characteristics. Even with a prolonged reaction time, no other thermal characteristics can be detected in these two samples. The low exothermic characteristics of MKLC0 and MKL0 pastes demonstrate their low degree of reaction and the slightest formation of gel. This suggests that without the addition of GGBFS, the geopolymerization reaction is significantly slowed or limited.

These heat release results indicate that the polymerization process is more influenced by the incorporation of GGBFS as a substitute for MKs in the formulations than by the reaction time. GGBFS appears to play a crucial role in accelerat-

ing dissolution and polymerization, leading to faster and more complete gel formation. This acceleration of the reaction may explain the improvements observed in the mechanical properties of geopolymers containing GGBFS.

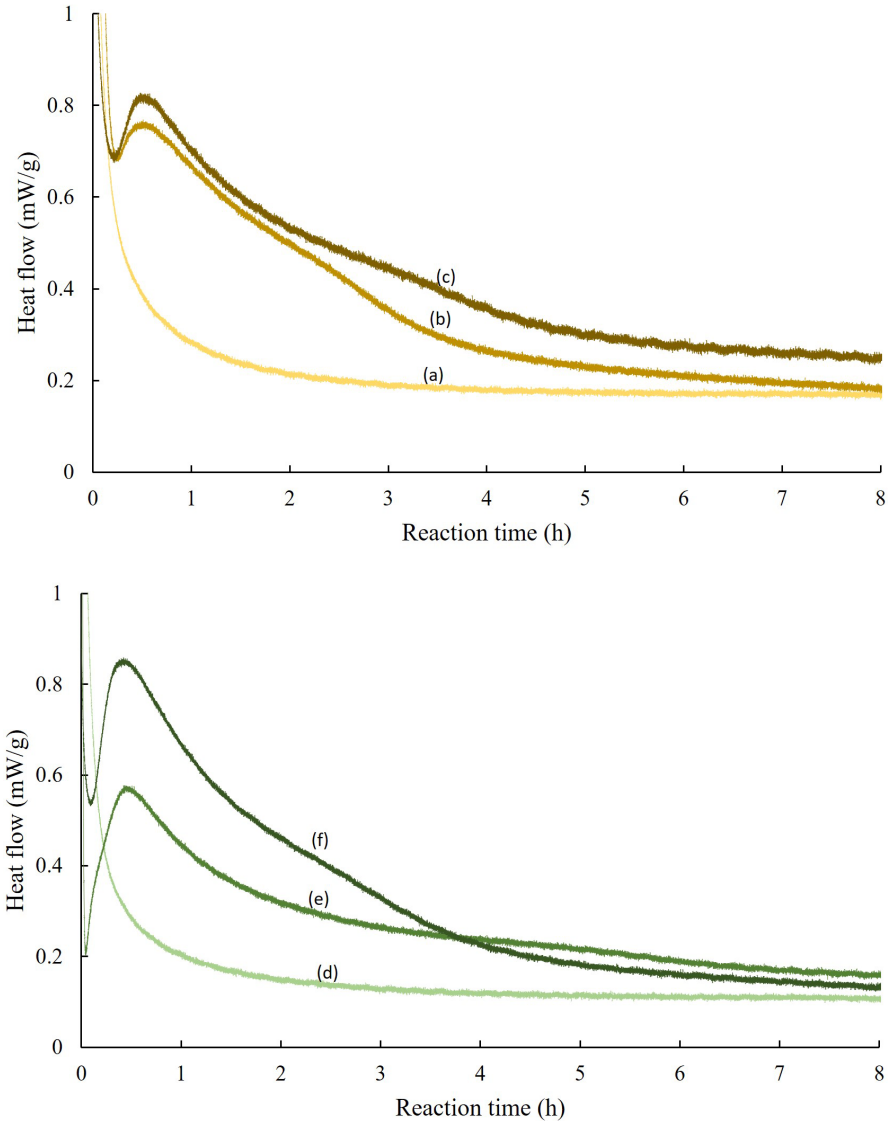

Figure 10. Heat release results of MKL0 (a), MKL5 (b), MKL10 (c), MKLC0 (d), MKLC5 (e) and MKLC10 (f).

4. Conclusions

This study focused on the valorization of clays and laterites of Burkina Faso in the formulation of geopolymers, with the main objective of evaluating the impact of the incorporation of granulated blast furnace dairy (GGBFS) on the geopolymerization of clay and laterite metakaolins. Several formulations have been developed and divided into three categories according to their composition: 100% MK without GGBFS, 95% MK and 5% GGBFS, and 90% MK and 10% GGBFS. The alkali/binder ratio was kept constant, and all formulations were hardened under the

same conditions. Compressive strength, mercury porosimetry and calorimetry tests were carried out, leading to the following results:

- Clay metakaolin-based geopolymers (MKC0), with a high theoretical molar ratio of SiO_2/Al_2O_3 of 2.83, had the lowest mechanical resistances (3 MPa) due to their highly crystalline nature. On the other hand, geopolymers based on laterite metakaolin (MKL0), with a theoretical molar ratio of 1.43, showed amorphous characteristics and mechanical resistances of up to 15 MPa, suggesting that the amorphous nature favors resistance.
- The increase in the amount of GGBFS resulted in a significant increase in compressive strength and a reduction in porosity. This suggests that GGBFS contributes to the formation of a denser and more compact microstructure, by forming C-A-S-H gel and filling gaps.
- The study of mercury porosimetry revealed that the increase in the level of GGBFS in the formulations improved porosity and mechanical strength. This indicates that the GGBFS acts as a densification agent, reducing porosity and strengthening the geopolymeric matrix.
- Calorimetry tests have highlighted the exothermic character of geopolymerization, demonstrating a strong correlation between heat release and compressive strength. The initial heat release, linked to the dissolution of the precursors, and the second peak, linked to polymerization, indicate a reaction kinetics accelerated by the addition of GGBFS, which results in better mechanical strength.

The results of this study demonstrate that clay and laterite-based geopolymer formulations have considerable mechanical potential, offering a credible alternative to ordinary Portland cement (OPC). Their adoption could play a key role in reducing the ecological footprint by limiting CO_2 emissions generated by the construction sector, while promoting the use of more sustainable and environmentally friendly materials. However, additional studies are needed to evaluate the long-term durability of these geopolymers under varying environmental conditions, as well as their shrinkage behavior and other mechanical constraints.

Acknowledgements

The authors would like to warmly thank the Service of Cooperation and Cultural Action of the French Embassy in Burkina Faso for their financial support for the mobility required for this study. We also express our sincere thanks to the team at the Civil Engineering and Geo-Environmental Laboratory (LGCgE) of IMT Nord Europe for their hospitality, scientific support, and the provision of their research facilities. Finally, we express our gratitude to the company Monitoring et Inspection/Structure et Environnement (MISE) for its valuable participation in establishing the relationships that made this study possible.

Declaration of Competing Interest

The authors declare that they have no known competing financial interests or personal relationships that could have appeared to influence the work reported in this paper.

References

[1] Eliang, J. (2023) UN Environment Programme. In: Idowu, S.O., Schmidpeter, R., Capaldi, N., Zu, L., Del Baldo, M. and Abreu, R., Eds., *Encyclopedia of Sustainable Management*, Springer, 3802. https://doi.org/10.1007/978-3-031-25984-5_302264.

[2] Benhelal, E., Zahedi, G., Shamsaei, E. and Bahadori, A. (2013) Global Strategies and Potentials to Curb CO_2 Emissions in Cement Industry. *Journal of Cleaner Production*, **51**, 142-161. https://doi.org/10.1016/j.jclepro.2012.10.049

[3] Mudgal, V. and Chellasamy, A. (2024) Growth of Indian Cement Industry, Its Environment Impact and Emerging Alternatives. *Indian Journal of Engineering and Materials Sciences*, **31**, 38-50.

[4] Singh, N.B., Kumar, M. and Rai, S. (2020) Geopolymer Cement and Concrete: Properties. *Materials Today*: *Proceedings*, **29**, 743-748. https://doi.org/10.1016/j.matpr.2020.04.513

[5] Okoye, F.N. (2017) Geopolymer Binder: A Veritable Alternative to Portland Cement. *Materials Today*: *Proceedings*, **4**, 5599-5604. https://doi.org/10.1016/j.matpr.2017.06.017

[6] Amar, M., Ladduri, B., Alloul, A., Benzerzour, M. and Abriak, N. (2024) Geopolymer Synthesis and Performance Paving the Way for Greener Building Material: A Comprehensive Study. *Case Studies in Construction Materials*, **20**, e03280. https://doi.org/10.1016/j.cscm.2024.e03280

[7] Chub-Uppakarn, T., Chompoorat, T., Thepumong, T., Sae-Long, W., Khamplod, A. and Chaiprapat, S. (2023) Influence of Partial Substitution of Metakaolin by Palm Oil Fuel Ash and Alumina Waste Ash on Compressive Strength and Microstructure in Metakaolin-Based Geopolymer Mortar. *Case Studies in Construction Materials*, **19**, e02519. https://doi.org/10.1016/j.cscm.2023.e02519

[8] Bajpai, R., Choudhary, K., Srivastava, A., Sangwan, K.S. and Singh, M. (2020) Environmental Impact Assessment of Fly Ash and Silica Fume Based Geopolymer Concrete. *Journal of Cleaner Production*, **254**, Article 120147. https://doi.org/10.1016/j.jclepro.2020.120147

[9] Wang, Q., Zhang, R., Xu, H., Li, M. and Fang, Z. (2023) Study on Mechanical Properties and Microstructure of Fly-Ash-Based Geopolymer for Solidifying Waste Mud. *Construction and Building Materials*, **409**, Article 134176. https://doi.org/10.1016/j.conbuildmat.2023.134176

[10] Jamil, N.H., Abdullah, M.M.A.B., Che Pa, F., Mohamad, H., W. Ibrahim, W.M.A. and Chaiprapa, J. (2020) Influences of SiO_2, Al_2O_3, CaO and MgO in Phase Transformation of Sintered Kaolin-Ground Granulated Blast Furnace Slag Geopolymer. *Journal of Materials Research and Technology*, **9**, 14922-14932. https://doi.org/10.1016/j.jmrt.2020.10.045

[11] Jamil, N., Abdullah, M., Ibrahim, W., Rahim, R., Sandu, A., Vizureanu, P., *et al.* (2022) Effect of Sintering Parameters on Microstructural Evolution of Low Sintered Geopolymer Based on Kaolin and Ground-Granulated Blast-Furnace Slag. *Crystals*, **12**, Article 1553. https://doi.org/10.3390/cryst12111553

[12] Abdullah, M.M.A.B., Ming, L.Y., Yong, H.C. and Tahir, M.F.M. (2018) Clay-Based Materials in Geopolymer Technology. In: Saleh, H.E.-D.M. and Rahman, R.O.A., Eds., *Cement Based Materials*, InTech, 239-264. https://doi.org/10.5772/intechopen.74438

[13] Vahab, N.A., Deepa, R.S. and Soman, M. (2024) A Review on Microstructural, Mechanical, and Durability Characteristics of Raw Kaolin Clay-Based Geopolymers. AIP Conference Proceedings, **3010**, Article 020006. https://doi.org/10.1063/5.0193543

[14] Lekshmi, S., Sudhakumar, J. and Thomas, S. (2023) Application of Clay in Geopolymer System: A State-of-the-Art Review. *Materials Today*: *Proceedings*, In Press. https://doi.org/10.1016/j.matpr.2023.04.083

[15] Nkwaju, R.Y., Nouping, J.N.F., Bachirou, S., Abo, T.M., Deutou, J.G.N. and Djobo, J.N.Y. (2023) Effective Stabilization of Cadmium and Copper in Iron-Rich Laterite-Based Geopolymers and Influence on Physical Properties. *Materials*, **16**, Article 7605. https://doi.org/10.3390/ma16247605

[16] Poudeu, R.C., Ekani, C.J., Djangang, C.N. and Blanchart, P. (2019) Role of Heat-Treated Laterite on the Strengthening of Geopolymer Designed with Laterite as Solid Precursor. *Annales de Chimie-Science des Matériaux*, **43**, 359-367. https://doi.org/10.18280/acsm.430601

[17] Tahmasebi Yamchelou, M., Law, D., Brkljača, R., Gunasekara, C., Li, J. and Patnaikuni, I. (2021) Geopolymer Synthesis Using Low-Grade Clays. *Construction and Building Materials*, **268**, Article 121066. https://doi.org/10.1016/j.conbuildmat.2020.121066

[18] Nana, A., Alomayri, T.S., Venyite, P., Kaze, R.C., Assaedi, H.S., Nobouassia, C.B., *et al.* (2022) Mechanical Properties and Microstructure of a Metakaolin-Based Inorganic Polymer Mortar Reinforced with Quartz Sand. *Silicon*, **14**, 263-274. https://doi.org/10.1007/s12633-020-00816-4

[19] Wyss, U. (2005) La construction en " matériaux locaux " état d'un secteur à potentiel multiple. Direction du Développement et de la Coopération Suisse, 77.

[20] Sore, S.O., Messan, A., Prud'homme, E., Escadeillas, G. and Tsobnang, F. (2016) Synthesis and Characterization of Geopolymer Binders Based on Local Materials from Burkina Faso—Metakaolin and Rice Husk Ash. *Construction and Building Materials*, **124**, 301-311. https://doi.org/10.1016/j.conbuildmat.2016.07.102

[21] Cyriaque Kaze, R., Naghizadeh, A., Tchadjie, L., Adesina, A., Noel Yankwa Djobo, J., Deutou Nemaleu, J.G., *et al.* (2022) Lateritic Soils Based Geopolymer Materials: A Review. *Construction and Building Materials*, **344**, Article 128157. https://doi.org/10.1016/j.conbuildmat.2022.128157

[22] Mathew, G. and Issac, B.M. (2020) Effect of Molarity of Sodium Hydroxide on the Aluminosilicate Content in Laterite Aggregate of Laterised Geopolymer Concrete. *Journal of Building Engineering*, **32**, Article 101486. https://doi.org/10.1016/j.jobe.2020.101486

[23] Alloul, A., Amar, M., Benzerzour, M. and Abriak, N. (2023) Geopolymer Mortar with Flash-Calcined Sediments Cured under Ambient Conditions. *Construction and Building Materials*, **391**, Article 131809. https://doi.org/10.1016/j.conbuildmat.2023.131809

[24] Alloul, A., Amar, M., Benzerzour, M. and Abriak, N. (2023) A Comparative Analysis of Ambient-Cured Metakaolin Geopolymer Mortar and Flash-Calcined Soil Geopolymer. *Construction and Building Materials*, **409**, Article 134085. https://doi.org/10.1016/j.conbuildmat.2023.134085

[25] (2016) Methods of Testing Cement. Part 1: Determination of Strength. AFNOR Editions. https://www.boutique.afnor.org/en-gb/standard/nf-en-1961/methods-of-testing-cement-part-1-determination-of-strength/fa184622/57803

[26] Bowles, J.F.W. (1997) R.M. Cornell and U. Schwertmann *The Iron Oxides*: *Structure*, *Properties Reactions Occurrence and Uses*. Weinheim and New York (VCH Verlagsgeseiischaft mbH). 1996, xxxi + 573 pp. Price DM 328.00. ISBN 3-527-28576-8. *Mineralogical Magazine*, **61**, 740-741. https://doi.org/10.1180/minmag.1997.061.408.20

[27] Dah-Traoré, Y., Zerbo, L., Seynou, M. and Ouedraogo, R. (2018) Mechanical, Microstructural and Mineralogical Analyses of Porous Clay Pots Elaborated with Rice Husks. *Journal of Minerals and Materials Characterization and Engineering*, **6**, 257-270. https://doi.org/10.4236/jmmce.2018.63019

[28] Sanou, S., Sanou, I., Ouedraogo, M., Bamogo, H., Gnoumou, L.V.L., Millogo, Y., *et al*. (2023) Stabilization of a Lateric Clay from Burkina Faso with Cement-Metakaolin for an Application in Road Construction. *Journal of Materials Science and Chemical Engineering*, **11**, 1-20. https://doi.org/10.4236/msce.2023.116001

[29] Ramadji, C., Messan, A., Sore, S.O., Prud'homme, E. and Nshimiyimana, P. (2022) Microstructural Analysis of the Reactivity Parameters of Calcined Clays. *Sustainability*, **14**, Article 2308. https://doi.org/10.3390/su14042308

[30] McKeown, D.A. (2005) Raman Spectroscopy and Vibrational Analyses of Albite: From 25 °C through the Melting Temperature. *American Mineralogist*, **90**, 1506-1517. https://doi.org/10.2138/am.2005.1726

[31] Seynou, M., Millogo, Y., Zerbo, L., Sanou, I., Ganon, F., Ouedraogo, R., *et al*. (2016) Production and Characterization of Pozzolan with Raw Clay from Burkina Faso. *Journal of Minerals and Materials Characterization and Engineering*, **4**, 195-209. https://doi.org/10.4236/jmmce.2016.43018

[32] Elimbi, A., Tchakoute, H.K., Kondoh, M. and Dika Manga, J. (2014) Thermal Behavior and Characteristics of Fired Geopolymers Produced from Local Cameroonian Metakaolin. *Ceramics International*, **40**, 4515-4520. https://doi.org/10.1016/j.ceramint.2013.08.126

[33] Tchakoute Kouamo, H., Elimbi, A., Mbey, J.A., Ngally Sabouang, C.J. and Njopwouo, D. (2012) The Effect of Adding Alumina-Oxide to Metakaolin and Volcanic Ash on Geopolymer Products: A Comparative Study. *Construction and Building Materials*, **35**, 960-969. https://doi.org/10.1016/j.conbuildmat.2012.04.023

[34] Finocchiaro, C., Barone, G., Mazzoleni, P., Leonelli, C., Gharzouni, A. and Rossignol, S. (2020) FT-IR Study of Early Stages of Alkali Activated Materials Based on Pyroclastic Deposits (Mt. Etna, Sicily, Italy) Using Two Different Alkaline Solutions. *Construction and Building Materials*, **262**, Article 120095. https://doi.org/10.1016/j.conbuildmat.2020.120095

[35] Emmerich, K. (2000) Spontaneous Rehydroxylation of a Dehydroxylated *Cis*-Vacant Montmorillonite. *Clays and Clay Minerals*, **48**, 405-408. https://doi.org/10.1346/ccmn.2000.0480312

[36] Castelein, O., Soulestin, B., Bonnet, J.P. and Blanchart, P. (2001) The Influence of Heating Rate on the Thermal Behaviour and Mullite Formation from a Kaolin Raw Material. *Ceramics International*, **27**, 517-522. https://doi.org/10.1016/s0272-8842(00)00110-3

[37] Wolska, E. and Schwertmann, U. (1989) Selective X-Ray Line Broadening in the Goethite-Derivedhematite Phase. *Physica Status Solidi* (*a*), **114**, K11-K16. https://doi.org/10.1002/pssa.2211140148

[38] Davidovits, J. (1991) Geopolymers. *Journal of Thermal Analysis*, **37**, 1633-1656. https://doi.org/10.1007/bf01912193

[39] Zhang, W., Hama, Y. and Na, S.H. (2015) Drying Shrinkage and Microstructure Characteristics of Mortar Incorporating Ground Granulated Blast Furnace Slag and Shrinkage Reducing Admixture. *Construction and Building Materials*, **93**, 267-277. https://doi.org/10.1016/j.conbuildmat.2015.05.103

[40] Ishikawa, K., Yoshioka, T., Sato, T. and Okuwaki, A. (1997) Solubility of Hematite in LioH, NaOH and KOH Solutions. *Hydrometallurgy*, **45**, 129-135. https://doi.org/10.1016/s0304-386x(96)00068-0

[41] Rathanasalam, V., Perumalsami, J. and Jayakumar, K. (2020) Characteristics of Blended Geopolymer Concrete Using Ultrafine Ground Granulated Blast Furnace Slag and Copper Slag. *Annales de Chimie-Science des Matériaux*, **44**, 433-439. https://doi.org/10.18280/acsm.440610

[42] Bernal, S.A., Rodríguez, E.D., Mejía de Gutiérrez, R., Gordillo, M. and Provis, J.L. (2011) Mechanical and Thermal Characterisation of Geopolymers Based on Silicate-Activated Metakaolin/Slag Blends. *Journal of Materials Science*, **46**, 5477-5486. https://doi.org/10.1007/s10853-011-5490-z

[43] Rodrigue Kaze, C., Ninla Lemougna, P., Alomayri, T., Assaedi, H., Adesina, A., Kumar Das, S., *et al.* (2021) Characterization and Performance Evaluation of Laterite Based Geopolymer Binder Cured at Different Temperatures. *Construction and Building Materials*, **270**, Article 121443. https://doi.org/10.1016/j.conbuildmat.2020.121443

[44] Steveson, M. and Sagoe-Crentsil, K. (2005) Relationships between Composition, Structure and Strength of Inorganic Polymers. *Journal of Materials Science*, **40**, 2023-2036. https://doi.org/10.1007/s10853-005-1226-2

[45] Ozer, I. and Soyer-Uzun, S. (2015) Relations between the Structural Characteristics and Compressive Strength in Metakaolin Based Geopolymers with Different Molar Si/Al Ratios. *Ceramics International*, **41**, 10192-10198. https://doi.org/10.1016/j.ceramint.2015.04.125

[46] Palomo, A., Blanco-Varela, M.T., Granizo, M.L., Puertas, F., Vazquez, T. and Grutzeck, M.W. (1999) Chemical Stability of Cementitious Materials Based on Metakaolin. *Cement and Concrete Research*, **29**, 997-1004. https://doi.org/10.1016/s0008-8846(99)00074-5

[47] Collins, F. and Sanjayan, J.G. (2001) Microcracking and Strength Development of Alkali Activated Slag Concrete. *Cement and Concrete Composites*, **23**, 345-352. https://doi.org/10.1016/s0958-9465(01)00003-8

[48] Duxson, P., Provis, J.L., Lukey, G.C. and van Deventer, J.S.J. (2007) The Role of Inorganic Polymer Technology in the Development of 'Green Concrete'. *Cement and Concrete Research*, **37**, 1590-1597. https://doi.org/10.1016/j.cemconres.2007.08.018

[49] Aiken, T.A., Kwasny, J., Sha, W. and Soutsos, M.N. (2018) Effect of Slag Content and Activator Dosage on the Resistance of Fly Ash Geopolymer Binders to Sulfuric Acid Attack. *Cement and Concrete Research*, **111**, 23-40. https://doi.org/10.1016/j.cemconres.2018.06.011

[50] Bekiaris, G., Peltre, C., Barsberg, S.T., Bruun, S., Sørensen, K.M., Engelsen, S.B., *et al.* (2020) Three Different Fourier-Transform Mid-Infrared Sampling Techniques to Characterize Bio-Organic Samples. *Journal of Environmental Quality*, **49**, 1310-1321. https://doi.org/10.1002/jeq2.20106

[51] Djobo, J.N.Y., Elimbi, A., Tchakouté, H.K. and Kumar, S. (2016) Reactivity of Volcanic Ash in Alkaline Medium, Microstructural and Strength Characteristics of Resulting Geopolymers under Different Synthesis Conditions. *Journal of Materials Science*, **51**, 10301-10317. https://doi.org/10.1007/s10853-016-0257-1

[52] Tchadjié, L.N., Djobo, J.N.Y., Ranjbar, N., Tchakouté, H.K., Kenne, B.B.D., Elimbi, A., *et al.* (2016) Potential of Using Granite Waste as Raw Material for Geopolymer Synthesis. *Ceramics International*, **42**, 3046-3055. https://doi.org/10.1016/j.ceramint.2015.10.091

[53] Robayo-Salazar, R.A., Mejía de Gutiérrez, R. and Puertas, F. (2016) Effect of Metakaolin on Natural Volcanic Pozzolan-Based Geopolymer Cement. *Applied Clay*

Science, **132**, 491-497. https://doi.org/10.1016/j.clay.2016.07.020

[54] Kalinkin, A.M., Gurevich, B.I., Myshenkov, M.S., Chislov, M.V., Kalinkina, E.V., Zvereva, I.A., *et al.* (2020) Synthesis of Fly Ash-Based Geopolymers: Effect of Calcite Addition and Mechanical Activation. *Minerals*, **10**, Article 827. https://doi.org/10.3390/min10090827

[55] Dupuy, C., Gharzouni, A., Sobrados, I., Tessier-Doyen, N., Texier-Mandoki, N., Bourbon, X., *et al.* (2020) Formulation of an Alkali-Activated Grout Based on Callovo-Oxfordian Argillite for an Application in Geological Radioactive Waste Disposal. *Construction and Building Materials*, **232**, Article 117170. https://doi.org/10.1016/j.conbuildmat.2019.117170

[56] Simão, L., Fernandes, E., Hotza, D., Ribeiro, M.J., Montedo, O.R.K. and Raupp-Pereira, F. (2021) Controlling Efflorescence in Geopolymers: A New Approach. *Case Studies in Construction Materials*, **15**, e00740. https://doi.org/10.1016/j.cscm.2021.e00740

[57] Provis, J.L. and Van Deventer, J.S.J. (2009) Geopolymers: Structures, Processing, Properties and Industrial Applications. Woodhead Publishing. https://doi.org/10.1533/9781845696382

[58] Shi, C., Roy, D. and Krivenko, P. (2003) Alkali-Activated Cements and Concretes. CRC Press. https://doi.org/10.1201/9781482266900.

[59] Liang, G., Liu, T., Li, H. and Wu, K. (2022) Shrinkage Mitigation, Strength Enhancement and Microstructure Improvement of Alkali-Activated Slag/Fly Ash Binders by Ultrafine Waste Concrete Powder. *Composites Part B*: *Engineering*, **231**, Article 109570. https://doi.org/10.1016/j.compositesb.2021.109570

[60] Sun, Z. and Vollpracht, A. (2018) Isothermal Calorimetry and In-Situ XRD Study of the NaOH Activated Fly Ash, Metakaolin and Slag. *Cement and Concrete Research*, **103**, 110-122. https://doi.org/10.1016/j.cemconres.2017.10.004

[61] Chithiraputhiran, S. and Neithalath, N. (2013) Isothermal Reaction Kinetics and Temperature Dependence of Alkali Activation of Slag, Fly Ash and Their Blends. *Construction and Building Materials*, **45**, 233-242. https://doi.org/10.1016/j.conbuildmat.2013.03.061

[62] Liang, G., Yao, W. and She, A. (2023) New Insights into the Early-Age Reaction Kinetics of Metakaolin Geopolymer by ^{1}H Low-Field NMR and Isothermal Calorimetry. *Cement and Concrete Composites*, **137**, Article 104932. https://doi.org/10.1016/j.cemconcomp.2023.104932

[63] Cai, J., Li, X., Tan, J. and Vandevyvere, B. (2020) Thermal and Compressive Behaviors of Fly Ash and Metakaolin-Based Geopolymer. *Journal of Building Engineering*, **30**, Article 101307. https://doi.org/10.1016/j.jobe.2020.101307

[64] Kumar, S., Kumar, R. and Mehrotra, S.P. (2010) Influence of Granulated Blast Furnace Slag on the Reaction, Structure and Properties of Fly Ash Based Geopolymer. *Journal of Materials Science*, **45**, 607-615. https://doi.org/10.1007/s10853-009-3934-5

[65] Yao, X., Zhang, Z., Zhu, H. and Chen, Y. (2009) Geopolymerization Process of Alkali-Metakaolinite Characterized by Isothermal Calorimetry. *Thermochimica Acta*, **493**, 49-54. https://doi.org/10.1016/j.tca.2009.04.002